INTERNATIONAL JOURNAL OF CIRCUITS, SYSTEMS AND SIGNAL PROCESSING
DOI: 10.46300/9106.2022.16.107 Volume 16, 2022

Bearings-only tracking based on distributed multisensor pseudolinear Kalman filter

Jungen Zhang, Shanglin Yang
North Minzu University,
204 Wenchang North Street, Yinchuan, Ningxia, 750021
China

Received: April 27, 2021. Revised: February 18, 2022. Accepted: March 9, 2022. Published: March 28, 2022.

Abstract—For bearings-only tracking (BOT), there are mainly two problems of nonlinear filtering and poor range observability. In the paper, a new distributed multisensor pseudolinear Kalman filter (PLKF) algorithm is proposed. The sensors use an instrumental vector PLKF (IV-PLKF) to process the measurements of the target independently, which can tackle the bias arising from the correlation between the measurement vector and pseudolinear noise by the bias compensation PLKF (BC-PLKF). The IV-PLKF embeds the recursive instrumental vector estimation method into the BC-PLKF, uses it to construct the instrumental vector, and applies the method of selective angle measurement to modify the local target state estimation and covariance. In the fusion center, the target state can be estimated by using the multisensor optimal information fusion criterion. Then the Cramer-Rao lower bound (CRLB) of multisensor BOT is derived. Simulation results show the effectiveness of the algorithm.

Keywords—pseudolinear Kalman filter, distributed multisensor, bearings-only tracking, instrumental vector, optimal information fusion.

I. INTRODUCTION

or many years, target tracking has been a hot research field, Fwhich is widely used in navigation, radar, sonar and wireless sensor networks. The goal of bearings-only tracking (BOT) is to estimate the target trajectory from the noisy target bearing data collected by a single motion sensor or multiple spatially distributed sensor nodes [1-3].

The challenge of BOT problem mainly comes from the nonlinearity of measurement equation and the lack of target radial distance observability. A straightforward application of the popular extended Kalman filter (EKF) to the BOT problem may produce unstable results. In order to improve the performance, some improved algorithms are proposed, such as MIEKF, MP-EKF and UKF [4-6]. Particle filter (PF) is an optimal nonlinear filter based on Monte Carlo integration. It is also applied to bearings-only target tracking [7]. One of the main disadvantages of PF is its high computational complexity, which limits its application in real-time target tracking [8]. For BOT, linearized recursive Bayesian estimation can be obtained by using pseudolinear equations instead of nonlinear bearing measurements. This method is usually called pseudolinear Kalman filter (PLKF) [9]. Compared with PF and other nonlinear Kalman filter algorithms (such as UKF), PLKF algorithm not only provides comparable tracking performance, but also requires lower computational complexity. In addition, PLKF has better robustness than EKF for the influence of initialization error, and has the same complexity as EKF. However, PLKF has a serious bias problem, and the tracking performance is inevitably affected by the relationship between relative geometry and motion [10]. In [11], the asymptotic bias of pseudolinear estimation of bearings only target motion is analyzed, and a bias compensation method based on instantaneous bias estimation is proposed. Of course, in order to increase accuracy, these pseudolinear estimation methods can be extended to a variety of mixed measurement information [12,13]. In [14], the noise is directly separated from the measurement vector and an unbiased PLKF algorithm is presented, which extends the PLKF to the maneuvering target tracking scene. In [15], the correlation between pseudo measurement matrix and pseudolinear noise is analyzed in detail, and a pseudolinear filter without bias compensation in the framework of minimum mean square error (MMSE) is proposed. These methods only consider the case of a single sensor.

Since a static sensor cannot track the target only by bearing measurement, in order to achieve full observability of the target state, the sensor needs to exert a specific maneuver, which is not desirable in some scene applications [16]. With multiple sensors, this issue does not exist, but the measurement data needs to be fused to obtain accurate estimation of target trajectory [17]. Generally, there are two different fusion structures. One is centralized fusion, in which all measurement data are sent to the central site for processing directly. The advantage is that the loss of information is minimal. The disadvantage is that the amount of data processed is too large,

resulting in serious computing load. The other is distributed fusion, where the local sensors yield global optimal or suboptimal state estimation by using specific information fusion rules. The advantage is that it is amenable for fully parallel implementation, which can improve the rate of input data and make fault detection and isolation easy [18]. In [19,20], the authors gives the optimal information fusion rule weighted by matrix in the sense of linear minimum variance (LMV), which is equivalent to the maximum likelihood (ML) fusion rule under the assumption of normal distribution. In [21], a general distributed optimal linear fusion estimation algorithm with matrix gain Kalman structure is proposed under the linear unbiased minimum variance criterion. In order to reduce the amount of computation, two suboptimal linear fusion estimation algorithms with diagonal matrix gain and scalar gain are proposed.

This paper combines the improved PLKF with the optimal fusion method, and proposes a distributed multisensor pseudolinear Kalman filter BOT algorithm. Each sensor subsystem processes the measurement value of the target independently, uses the instrumental vector PLKF for filtering estimation, sends the local target state estimation to the fusion center, in which the multisensor optimal information fusion criterion is used and the fusion estimation of the target state can be obtained. In addition, the calculation method of Cramer-Rao lower bound (CRLB) of multisensor BOT is presented. Finally, the effectiveness of the algorithm is verified by simulation experiments.

This paper is organized as follows. In Section II, the formulation of the multisensor BOT problem is presented and the PLKF is reviewed briefly. In Section III, the proposed distributed multisensor pseudolinear Kalman filter BOT algorithm is described in detail and the CRLB for the BOT problem is derived. In Section IV, the simulation results and performance analysis of the proposed BOT algorithm are given. And finally, some conclusions are summarized in Section V.

II. Problem Formulation

A. Multisensor BOT problem

Consider the following multisensor BOT system:

$$\mathbf{x}_{k+1} = \mathbf{F}\mathbf{x}_k + \mathbf{w}_k \tag{1}$$

$$\boldsymbol{\theta}_k = h\left(\mathbf{x}_k\right) + \mathbf{v}_k \tag{2}$$

where $\mathbf{x}_k = \left[x_k, x_k, y_k, y_k\right]^{\mathrm{T}}$ is the target state vector at time k, $[\cdot]^{\mathrm{T}}$ denotes the transpose of $[\cdot]$, $\mathbf{F}$ is the state transition matrix, $\mathbf{F} = \mathrm{diag}\left(\left[\mathbf{F}, \mathbf{F}\right]\right)$, $\mathbf{F} = \begin{bmatrix} 1 & T_s \\ 0 & 1 \end{bmatrix}$, $\mathrm{diag}(\cdot)$ denotes diagonal matrix, T_s is the sampling period, $\mathbf{w}_k$ is a zero-mean white Gaussian noise with covariance matrix $\mathbf{Q}$, $\mathbf{Q} = \sigma \times \mathrm{diag}\left(\left[\mathbf{Q}, \mathbf{Q}\right]\right)$, $\mathbf{Q} = \begin{bmatrix} T_s^3/3 & T_s^2/2 \\ T_s^2/2 & T_s \end{bmatrix}$, σ is the power spectral density of process noise. $\boldsymbol{\theta}_k = \left[\theta_{1,k}, \mathrm{L}\ , \theta_{N_o,k}\right]^{\mathrm{T}}$, N_o is the number of sensors, $\theta_{n,k}$ is the target bearing generated by sensor n at time k. $\theta_{n,k} = \theta_{n,k} + v_{n,k}$, $\theta_{n,k} = \arctan\left(\dfrac{y(k) - r_y^n}{x(k) - r_x^n}\right)$, $n \in \left\{1, \mathrm{L}\ , N_o\right\}$, $\left(r_x^n, r_y^n\right)$ is the location of sensor n. The measurement noise $\mathbf{v}_{n,k}$ is a zero-mean white Gaussian process with covariance matrix σ_n^2. $\mathbf{v}_k = \left[v_{1,k}, \mathrm{L}\ , v_{N_o,k}\right]^{\mathrm{T}}$, and it is uncorrelated with process noise $\mathbf{w}_k$.

The target bearing $\boldsymbol{\theta}_k$ is a nonlinear function of the state vector $\mathbf{x}_k$, thereby making (1) and (2) a nonlinear state space model. Target tracking is to estimate the target state $\mathbf{x}_k$ from a history of bearing measurements up to time k.

B. PLKF

In order to apply Kalman filter to the state space model in BOT, the measurement equation (2) must be linearized. The EKF can achieve this by truncating Taylor series expansion. However, this can lead to some instability problems. A more attractive method is the pseudolinear estimation.

For a sensor, the bearing measurement equation can be written as

$$\frac{\sin\left(\theta_k - v_k\right)}{\cos\left(\theta_k - v_k\right)} = \frac{\mathrm{V}y_k}{\mathrm{V}x_k} \tag{3}$$

where $\mathrm{V}y_k = y_k - r_y^n$, $\mathrm{V}x_k = x_k - r_x^n$.

After several algebraic operations, the following pseudolinear equation is obtained.

$$\mathbf{u}_k^{\mathrm{T}}\mathbf{r} = \mathbf{u}_k^{\mathrm{T}}\mathbf{M}\mathbf{x}_k + \eta_k \tag{4}$$

where $\mathbf{u}_k = \begin{bmatrix} \sin\theta_k \\ -\cos\theta_k \end{bmatrix}$, $\mathbf{M} = \begin{bmatrix} 1 & 0 & 0 & 0 \\ 0 & 1 & 0 & 0 \end{bmatrix}$, $\mathbf{r} = \left[r_x^n, r_y^n\right]^{\mathrm{T}}$, $\eta_k = -\left\|\mathbf{d}_k\right\| \sin v_k$, $\left\|\mathbf{d}_k\right\|$ is the Euclidean distance from the sensor to the target. Letting $z_k = \mathbf{u}_k^{\mathrm{T}}\mathbf{r}$, $\mathbf{H}_k = \mathbf{u}_k^{\mathrm{T}}\mathbf{M}$, then the pseudolinear measurement equation can be rewritten as

$$z_k = \mathbf{H}_k\mathbf{x}_k + \eta_k \tag{5}$$

The variance of pseudolinear measurement noise η_k is R_k, which can be obtained by definition.

$$R_k = \mathrm{E}\left\{\eta_k^2\right\} = \left\|\mathbf{d}_k\right\|^2 \mu_k^2 \tag{6}$$

$$\mu_k^2=\mathrm{E}\left\{\sin^2 v_k\right\}=\frac{1}{2}\left(1-\exp\left(-2\sigma_n^2\right)\right) \tag{7}$$

For suffifiiciently small bearing measurement noise, $\mu_k^2 \approx \sigma_n^2$, R_k is given as $R_k \approx \left\|\mathbf{d}_k\right\|^2 \sigma_n^2$.

Equations (1) and (5) form a pseudolinear state target tracking model, and the target state is estimated by PLKF.

- State prediction:

$$\hat{\mathbf{x}}_{k|k-1}=\mathbf{F}\hat{\mathbf{x}}_{k-1|k-1} \tag{8}$$

- Calculation of the covariance of the predicted state:

$$\mathbf{P}_{k|k-1}=\mathbf{F}\mathbf{P}_{k-1|k-1}\mathbf{F}^{\mathrm{T}}+\mathbf{Q} \tag{9}$$

- Calculation of pseudolinear measurement noise variance:

$$R_k \approx \left\|\hat{\mathbf{d}}_{k|k-1}\right\|^2 \mu_k^2 \tag{10}$$

where $\hat{\mathbf{d}}_{k|k-1}=\mathbf{M}\hat{\mathbf{x}}_{k|k-1}-\mathbf{r}$.

- Calculate Kalman gain as:

$$\mathbf{K}_k=\mathbf{P}_{k|k-1}\mathbf{H}_k^{\mathrm{T}}\left(R_k+\mathbf{H}_k\mathbf{P}_{k|k-1}\mathbf{H}_k^{\mathrm{T}}\right)^{-1} \tag{11}$$

- State update:

$$\hat{\mathbf{x}}_{k|k}=\hat{\mathbf{x}}_{k|k-1}+\mathbf{K}_k\left(z_k-\mathbf{H}_k\hat{\mathbf{x}}_{k|k-1}\right) \tag{12}$$

- State covariance update:

$$\mathbf{P}_{k|k}=\left(\mathbf{I}-\mathbf{K}_k\mathbf{H}_k\right)\mathbf{P}_{k|k-1} \tag{13}$$

Different from the traditional linear state space model, in the pseudolinear measurement equation (5), the measurement vector $\mathbf{H}_k$ is correlated with the pseudo measurement noise η_k, and $\mathbf{H}_k$ is also a function of the state vector $\mathbf{x}_k$. This will lead to a bias problem in the PLKF, which will become significant when the process noise is large.

III. The Proposed Distributed Multisensor Pseudolinear Kalman Filter Algorithm

Firstly, the bias compensation PLKF is briefly described, and then the instrumental vector PLKF is introduced. For each distributed sensor subsystem, the IVPLKF is used to estimate the target state independently. The estimated target state and its covariance are sent to the fusion center. The fusion estimation of the target state is obtained by using the optimal information fusion criterion. Finally, the CRLB of multisensor BOT is deduced theoretically.

A. Bias compensation PLKF

The bias in PLKF is expressed as

$$\boldsymbol{\delta}_k=\mathrm{E}\left\{\hat{\mathbf{x}}_{k|k}-\mathbf{x}_k\right\}=\mathrm{E}\left\{\mathbf{A}_k\right\}+\mathrm{E}\left\{\mathbf{B}_k\right\}+\mathrm{E}\left\{\mathbf{C}_k\right\} \tag{14}$$

$$\mathbf{A}_k=\left(\mathbf{P}_{k|k-1}^{-1}+\mathbf{H}_k^{\mathrm{T}}R_k^{-1}\mathbf{H}_k\right)^{-1}\mathbf{P}_{k|k-1}^{-1}\mathbf{F}\left(\hat{\mathbf{x}}_{k-1|k-1}-\mathbf{x}_{k-1}\right) \tag{15}$$

$$\mathbf{B}_k=-\left(\mathbf{P}_{k|k-1}^{-1}+\mathbf{H}_k^{\mathrm{T}}R_k^{-1}\mathbf{H}_k\right)^{-1}\mathbf{P}_{k|k-1}^{-1}\mathbf{F}\mathbf{w}_{k-1} \tag{16}$$

$$\mathbf{C}_k=\left(\mathbf{P}_{k|k-1}^{-1}+\mathbf{H}_k^{\mathrm{T}}R_k^{-1}\mathbf{H}_k\right)^{-1}\mathbf{H}_k^{\mathrm{T}}R_k^{-1}\eta_k \tag{17}$$

For the bias term in equation (14), the first term $\mathrm{E}\left\{\mathbf{A}_k\right\}$ only propagates the bias at the previous time, so it is not the cause of the bias. In the second term, $\mathbf{H}_k$ is correlated with the process noise $\mathbf{w}_k$ because $\mathbf{H}_k$ is a function of $\mathbf{x}_k$. If the target moves at nearly constant velocity, the process noise is quite small, and the correlation between $\mathbf{H}_k$ and $\mathbf{w}_k$ will be weak. Therefore, $\left(\mathbf{P}_{k|k-1}^{-1}+\mathbf{H}_k^{\mathrm{T}}R_k^{-1}\mathbf{H}_k\right)^{-1}\mathbf{P}_{k|k-1}^{-1}$ is weakly correlated with $\mathbf{w}_k$. Then it can obtained as $\mathrm{E}\left\{\mathbf{B}_k\right\}\approx 0$. For the third term, $\mathrm{E}\left\{\mathbf{C}_k\right\}\neq 0$, because $\mathbf{H}_k$ and η_k are related by measurement noise $\mathbf{v}_k$. Therefore, for the nearly constant velocity target motion model, the root cause of state estimation bias in PLKF is the correlation between $\mathbf{H}_k$ and η_k. By compensating the bias caused by $\mathbf{C}_k$, the PLKF bias can be alleviated.

$\mathbf{C}_k$ can be calculated approximately:

$$\begin{aligned}\hat{\mathbf{C}}_k&=\left(\mathbf{P}_{k|k-1}^{-1}+\mathbf{H}_k^{\mathrm{T}}R_k^{-1}\mathbf{H}_k\right)^{-1}R_k^{-1}\mathrm{E}\left\{\mathbf{H}_k^{\mathrm{T}}\eta_k\left|\mathbf{x}_k\right.\right\}\\&=-\left(\mathbf{P}_{k|k-1}^{-1}+\mathbf{H}_k^{\mathrm{T}}R_k^{-1}\mathbf{H}_k\right)^{-1}R_k^{-1}\mu_k^2\mathbf{M}^{\mathrm{T}}\left(\mathbf{M}\hat{\mathbf{x}}_{k|k}-\mathbf{r}\right)\end{aligned} \tag{18}$$

The BC-PLKF method, that is, the instantaneous bias estimation of $\mathbf{C}_k$ is subtracted from $\hat{\mathbf{x}}_{k|k}$ estimated by PLKF to obtain the state estimation $\hat{\mathbf{x}}_{k|k}^{\mathrm{B}}$.

$$\begin{aligned}\hat{\mathbf{x}}_{k|k}^{\mathrm{B}}&=\hat{\mathbf{x}}_{k|k}-\hat{\mathbf{C}}_k\\&=\hat{\mathbf{x}}_{k|k}+\left(\mathbf{P}_{k|k-1}^{-1}+\mathbf{H}_k^{\mathrm{T}}R_k^{-1}\mathbf{H}_k\right)^{-1}R_k^{-1}\mu_k^2\mathbf{M}^{\mathrm{T}}\left(\mathbf{M}\hat{\mathbf{x}}_{k|k}-\mathbf{r}\right)\\&=\hat{\mathbf{x}}_{k|k}+\mathbf{P}_{k|k}R_k^{-1}\mu_k^2\mathbf{M}^{\mathrm{T}}\left(\mathbf{M}\hat{\mathbf{x}}_{k|k}-\mathbf{r}\right)\end{aligned} \tag{19}$$

B. Instrumental vector PLKF

Unlike the bias compensation PLKF, the instrumental vector PLKF aims to remove the bias due to $\mathbf{C}_k$ by eliminating the correlation between $\mathbf{H}_k$ and η_k, rather than directly subtracting $\mathbf{C}_k$ from the state estimation $\hat{\mathbf{x}}_{k|k}$.

The instrumental vector $\mathbf{G}_k$ is constructed with $\mathrm{E}\left\{\mathbf{G}_k^{\mathrm{T}}\eta_k\right\}=0$. The bias term caused by $\mathbf{C}_k$ in equation (14) can be approximately calculated for a sufficiently large k.

$$\mathrm{E}\left\{\mathbf{C}_k\right\}\approx\mathrm{E}\left\{\left(\mathbf{P}_{k|k-1}^{-1}+\mathbf{G}_k^{\mathrm{T}}R_k^{-1}\mathbf{H}_k\right)^{-1}R_k^{-1}\right\}\mathrm{E}\left\{\mathbf{G}_k^{\mathrm{T}}\eta_k\right\}\approx 0 \tag{20}$$

Thus, the approximate unbiased estimation of state estimation $\hat{\mathbf{x}}_{k|k}$ is obtained. The optimal choice of instrumental vector $\mathbf{G}_k$ can be given by the noiseless form of measurement

vector $\mathbf{H}_k$. Since the true target bearing θ_k is unknown, the suboptimal instrumental vector $\mathbf{G}_k$ can be given by replacing θ_k with the estimated value $\hat{\theta}_{k|k}^{\mathrm{B}}$ computed from bias compensation PLKF.

$$\mathbf{G}_k = \left[\sin\hat{\theta}_{k|k}^{\mathrm{B}}, -\cos\hat{\theta}_{k|k}^{\mathrm{B}}\right]\mathbf{M} \tag{21}$$

$$\hat{\theta}_{k|k}^{\mathrm{B}} = \arctan\left(\frac{\hat{\mathbf{x}}_{k|k}^{\mathrm{B}}(3) - r_y^n}{\hat{\mathbf{x}}_{k|k}^{\mathrm{B}}(1) - r_x^n}\right) \tag{22}$$

The instrumental vector $\mathbf{G}_k$ is required to have a strong correlation with the measurement vector $\mathbf{H}_k$. In the presence of large measurement noise and in unfavorable geometric measurement position, due to the large bias between the measured bearing $\theta_k^{\%}$ and the estimated bearing $\hat{\theta}_{k|k}^{\mathrm{B}}$, the correlation between $\mathbf{G}_k$ and $\mathbf{H}_k$ may be weakened, resulting in the poor performance of the target estimation. In order to maintain the strong correlation between $\mathbf{G}_k$ and $\mathbf{H}_k$, the selective angle measurement (SAM) strategy is combined into the instrumental vector PLKF algorithm.

If $\left|\hat{\theta}_{k|k}^{\mathrm{B}} - \theta_k^{\%}\right| < \alpha_k$ ($\alpha_k = \varepsilon\sigma_n$, where ε is a scalar factor), the instrumental vector is used to correct the target state estimation and covariance.

a. Calculate instrumental vector:

$$\mathbf{G}_k = \left[\sin\hat{\theta}_{k|k}^{\mathrm{B}}, -\cos\hat{\theta}_{k|k}^{\mathrm{B}}\right]\mathbf{M} \tag{23}$$

b. Gain correction:

$$\mathbf{K}_k^{\mathrm{IV}} = \mathbf{P}_{k|k-1}\mathbf{G}_k^{\mathrm{T}}\left(R_k + \mathbf{H}_k\mathbf{P}_{k|k-1}\mathbf{G}_k^{\mathrm{T}}\right)^{-1} \tag{24}$$

c. State correction:

$$\hat{\mathbf{x}}_{k|k}^{\mathrm{IV}} = \hat{\mathbf{x}}_{k|k-1} + \mathbf{K}_k^{\mathrm{IV}}\left(\mathbf{z}_k - \mathbf{H}_k\hat{\mathbf{x}}_{k|k-1}\right) \tag{25}$$

d. Covariance correction:

$$\mathbf{P}_{k|k}^{\mathrm{IV}} = \left(\mathbf{I} - \mathbf{K}_k^{\mathrm{IV}}\mathbf{H}_k\right)\mathbf{P}_{k|k-1} \tag{26}$$

C. Proposed distributed multisensor IVPLKF algorithm

In the distributed multisensor system, each sensor subsystem independently estimates the target state, sends the target state estimation and its covariance to the fusion center, where the optimal information fusion criterion is used to obtain the fusion estimation of the target state.

Assuming that the state estimation at time k obtained by multisensor is $\left[\hat{\mathbf{x}}_k^1, \mathrm{L}\ , \hat{\mathbf{x}}_k^{N_o}\right]$, the optimal fusion estimation of target state $\hat{\mathbf{x}}_k$ is given as:

$$\hat{\mathbf{x}}_k = \bar{\mathbf{A}}^1\hat{\mathbf{x}}_k^1 + \bar{\mathbf{A}}^2\hat{\mathbf{x}}_k^2 + \mathrm{L}\ + \bar{\mathbf{A}}^{N_o}\hat{\mathbf{x}}_k^{N_o} \tag{27}$$

In equation (35), $\bar{\mathbf{A}}^n$ is weight matrix, $n = 1, \mathrm{L}\ , N_o$.

$$\bar{\mathbf{A}} = \mathbf{\Sigma}^{-1}\mathbf{e}\left(\mathbf{e}^{\mathrm{T}}\mathbf{\Sigma}^{-1}\mathbf{e}\right)^{-1} \tag{28}$$

where $\mathbf{\Sigma} = \mathrm{diag}\left(\left[\mathbf{P}_k^1, \mathrm{L}\ , \mathbf{P}_k^{N_o}\right]\right)$ is a $4N_o \times 4N_o$ diagonal matrix, $\bar{\mathbf{A}} = \left[\bar{A}^1, \mathrm{L}\ , \bar{A}^{N_o}\right]^{\mathrm{T}}$, $\mathbf{e} = \left[\mathbf{I}_4, \mathrm{L}\ , \mathbf{I}_4\right]^{\mathrm{T}}$ is a $4N_o \times 4$ matrix, $\mathbf{I}_4$ is a 4×4 identity matrix. The covariance of the target state estimation is calculated as:

$$\mathbf{P}_k = \left(\mathbf{e}^{\mathrm{T}}\mathbf{\Sigma}^{-1}\mathbf{e}\right)^{-1} \tag{29}$$

Starting from the posterior target state estimation corresponding to sensor n at scan k, represented by $\hat{\mathbf{x}}_{k-1|k-1}^n$ and $\mathbf{P}_{k-1|k-1}^n$, a cycle of the proposed distributed multisensor IVPLKF (DM-IVPLKF) algorithm is summarized in Algorithm 1.

Algorithm 1: The proposed DM-IVPLKF algorithm

1: Input: $\hat{\mathbf{x}}_{k-1|k-1}^n$ and $\mathbf{P}_{k-1|k-1}^n$, $n \in 1, \mathrm{L}\ , N_o$.

2: Predict state $\hat{\mathbf{x}}_{k|k-1}^n$ according to (8).

3: Calculate the covariance of the predicted state $\mathbf{P}_{k|k-1}^n$ according to (9).

4: Calculate the pseudolinear measurement noise variance R_k^n according to (10).

5: Calculate gain $\mathbf{K}_k^n$ according to (11).

6: Update state $\hat{\mathbf{x}}_{k|k}^n$ according to (12).

7: Calculate the covariance of the update state $\mathbf{P}_{k|k}^n$ according to (13).

8: Calculate bias compensation estimation $\hat{\mathbf{x}}_{k|k}^{\mathrm{B},n}$ according to (19).

9: Estimate target bearing $\hat{\theta}_{k|k}^{\mathrm{B},n}$ according to (22).

10: Apply SAM strategy: If $\left|\hat{\theta}_{k|k}^{\mathrm{B}} - \theta_k^{\%}\right| < \alpha_k$, correct state $\hat{\mathbf{x}}_{k|k}^{\mathrm{IV},n}$ and covariance $\mathbf{P}_{k|k}^{\mathrm{IV},n}$ according to (25) and (26) respectively. Set $\hat{\mathbf{x}}_{k|k}^n = \hat{\mathbf{x}}_{k|k}^{\mathrm{IV},n}$ and $\mathbf{P}_{k|k}^n = \mathbf{P}_{k|k}^{\mathrm{IV},n}$. Otherwise, Set $\hat{\mathbf{x}}_{k|k}^n = \hat{\mathbf{x}}_{k|k}^{\mathrm{B},n}$.

11: Calculate fusion state $\hat{\mathbf{x}}_k$ and covariance $\mathbf{P}_k$ according to (27) and (29) respectively.

12: Output: $\hat{\mathbf{x}}_k$, $\mathbf{P}_k$.

D. The CRLB for multisensor BOT

As far as performance analysis is concerned, the CRLB is widely used to assess the performance of filters [9]. In the section, a theoretical CRLB for the multisensor BOT problem

is derived. For the filtering problem described in equations (1) and (2), a recursive formula is proposed for the Fisher information matrix inverse noted by $\mathbf{J}_k^{-1}$, which gives the CRLB as:

$$\mathbf{J}_{k+1} = \mathbf{D}_k^{22} - \mathbf{D}_k^{21}\left(\mathbf{J}_k + \mathbf{D}_k^{11}\right)^{-1}\mathbf{D}_k^{12} \tag{30}$$

where $\mathbf{D}_k^{11}$, $\mathbf{D}_k^{12}$, $\mathbf{D}_k^{21}$ and $\mathbf{D}_k^{22}$ are respectively defined as follows:

$$\mathbf{D}_k^{11} = -\mathrm{E}\left\{\nabla_{\mathbf{x}_k}\left[\nabla_{\mathbf{x}_k}\log p\left(\mathbf{x}_{k+1}\,|\,\mathbf{x}_k\right)\right]^{\mathrm{T}}\right\} \tag{31}$$

$$\mathbf{D}_k^{21} = -\mathrm{E}\left\{\nabla_{\mathbf{x}_k}\left[\nabla_{\mathbf{x}_{k+1}}\log p\left(\mathbf{x}_{k+1}\,|\,\mathbf{x}_k\right)\right]^{\mathrm{T}}\right\} \tag{32}$$

$$\mathbf{D}_k^{12} = -\mathrm{E}\left\{\nabla_{\mathbf{x}_{k+1}}\left[\nabla_{\mathbf{x}_k}\log p\left(\mathbf{x}_{k+1}\,|\,\mathbf{x}_k\right)\right]^{\mathrm{T}}\right\} = \left[\mathbf{D}_k^{21}\right]^{\mathrm{T}} \tag{33}$$

$$\begin{aligned}\mathbf{D}_k^{22} = &-\mathrm{E}\left\{\nabla_{\mathbf{x}_{k+1}}\left[\nabla_{\mathbf{x}_{k+1}}\log p\left(\mathbf{x}_{k+1}\,|\,\mathbf{x}_k\right)\right]^{\mathrm{T}}\right\}\\ &-\mathrm{E}\left\{\nabla_{\mathbf{x}_{k+1}}\left[\nabla_{\mathbf{x}_{k+1}}\log p\left(\mathbf{z}_{k+1}\,|\,\mathbf{x}_{k+1}\right)\right]^{\mathrm{T}}\right\}\end{aligned} \tag{34}$$

where ∇ denotes the gradient operator.

For the state equation (1), the calculation of $\mathbf{D}_k^{11}$ and $\mathbf{D}_k^{12}$ can be simplified as follows:

$$\begin{aligned}\mathbf{D}_k^{11} &= \mathrm{E}\{\nabla_{\mathbf{x}_k}\log p\left(\mathbf{x}_{k+1}\,|\,\mathbf{x}_k\right)[\nabla_{\mathbf{x}_k}\log p\left(\mathbf{x}_{k+1}\,|\,\mathbf{x}_k\right)]^{\mathrm{T}}\}\\ &= \mathbf{F}^{\mathrm{T}}\mathbf{Q}^{-1}\mathbf{F}\end{aligned} \tag{35}$$

$$\begin{aligned}\mathbf{D}_k^{12} &= \mathrm{E}\{\nabla_{\mathbf{x}_k}\log p\left(\mathbf{x}_{k+1}\,|\,\mathbf{x}_k\right)[\nabla_{\mathbf{x}_{k+1}}\log p\left(\mathbf{x}_{k+1}\,|\,\mathbf{x}_k\right)]^{\mathrm{T}}\}\\ &= -\mathbf{F}^{\mathrm{T}}\mathbf{Q}^{-1}\end{aligned} \tag{36}$$

Assuming that each sensor independently observes the target and the measured bearing is synchronous, $\mathbf{D}_k^{22}$ in equation (34) can be calculated by the following equation:

$$\begin{aligned}\mathbf{D}_k^{22} &= \mathrm{E}\{\nabla_{\mathbf{x}_{k+1}}\log p\left(\mathbf{x}_{k+1}\,|\,\mathbf{x}_k\right)[\nabla_{\mathbf{x}_{k+1}}\log p\left(\mathbf{x}_{k+1}\,|\,\mathbf{x}_k\right)]^{\mathrm{T}}\}\\ &+\mathrm{E}\{\nabla_{\mathbf{x}_{k+1}}\log p\left(\mathbf{z}_{k+1}\,|\,\mathbf{x}_{k+1}\right)[\nabla_{\mathbf{x}_{k+1}}\log p\left(\mathbf{z}_{k+1}\,|\,\mathbf{x}_{k+1}\right)]^{\mathrm{T}}\}\\ &= \mathbf{Q}^{-1} + \mathrm{E}\left\{\left(\mathbf{H}_{k+1}\right)^{\mathrm{T}}\mathbf{R}^{-1}\mathbf{H}_{k+1}\right\}\end{aligned} \tag{37}$$

where

$$\mathbf{H}_{k+1} = \left[\nabla_{\mathbf{x}_{k+1}}h\left(\mathbf{x}_{k+1}\right)\right]^{\mathrm{T}} \tag{38}$$

$$\mathbf{R} = \mathrm{diag}\left(\left[\sigma_1^2,\mathrm{L}\ ,\sigma_{N_o}^2\right]\right) \tag{39}$$

In equation (38), $\mathbf{H}_{k+1}$ can be obtained by calculating the gradient.

$$\mathbf{H}_{k+1} = \begin{bmatrix} \frac{\partial h_1}{\partial x_{k+1}} & \frac{\partial h_1}{\partial \dot{x}_{k+1}} & \frac{\partial h_1}{\partial y_{k+1}} & \frac{\partial h_1}{\partial \dot{y}_{k+1}} \\ \frac{\partial h_2}{\partial x_{k+1}} & \frac{\partial h_2}{\partial \dot{x}_{k+1}} & \frac{\partial h_2}{\partial y_{k+1}} & \frac{\partial h_2}{\partial \dot{y}_{k+1}} \\ \mathrm{M} & \mathrm{M} & \mathrm{M} & \mathrm{M} \\ \frac{\partial h_{N_o}}{\partial x_{k+1}} & \frac{\partial h_{N_o}}{\partial \dot{x}_{k+1}} & \frac{\partial h_{N_o}}{\partial y_{k+1}} & \frac{\partial h_{N_o}}{\partial \dot{y}_{k+1}} \end{bmatrix} \tag{40}$$

$$\frac{\partial h_n}{\partial x_{k+1}} = \frac{-\left(y_{k+1} - r_y^n\right)}{\left(y_{k+1} - r_y^n\right)^2 + \left(x_{k+1} - r_x^n\right)^2} \tag{41}$$

$$\frac{\partial h_n}{\partial y_{k+1}} = \frac{x_{k+1} - r_x^n}{\left(y_{k+1} - r_y^n\right)^2 + \left(x_{k+1} - r_x^n\right)^2} \tag{42}$$

$$\frac{\partial h_n}{\partial \dot{x}_{k+1}} = \frac{\partial h_n}{\partial \dot{y}_{k+1}} = 0\ ,\quad n = 1,\mathrm{L}\ ,N_o \tag{43}$$

The substitutions of equations (35), (36) and (37) into the recursion equation (30) yields:

$$\begin{aligned}\mathbf{J}_{k+1} = &\mathbf{Q}^{-1} + \mathrm{E}\left\{\left(\mathbf{H}_{k+1}\right)^{\mathrm{T}}\mathbf{R}^{-1}\mathbf{H}_{k+1}\right\}\\ &-\left(\mathbf{Q}^{-1}\right)^{\mathrm{T}}\mathbf{F}\left(\mathbf{J}_k + \mathbf{F}^{\mathrm{T}}\mathbf{Q}^{-1}\mathbf{F}\right)^{-1}\mathbf{F}^{\mathrm{T}}\mathbf{Q}^{-1}\end{aligned} \tag{44}$$

where the expectation operator E can be approximately calculated by Monte Carlo method.

IV. Simulation Results

This section presents a performance evaluation of the proposed distributed multisensor IVPLKF (DM-IVPLKF) algorithm in comparison to the DM-IPLKF, DM-PLKF, DM-EKF, DM-IEKF and DM-UKF algorithms using Monte-Carlo (MC) simulations. And the CRLB will be used to indicate the best possible performance that one can expect for a given scenario. Consider the distributed multisensor BOT model described in equations (1) and (2). The numerical values of the parameters of the dynamic system are given as follows.

$\mathbf{x}_0 = \left[0\mathrm{km}, 0.15\mathrm{km/s}, 23\mathrm{km}, 0.1\mathrm{km/s}\right]^{\mathrm{T}}$ is initial target state.

Number of sensors $N_o = 3$. The sensors are located at $(20,20)\,\mathrm{km}$, $(30,20)\,\mathrm{km}$ and $(25,28.66)\,\mathrm{km}$.

Sampling period $T_s = 1\mathrm{s}$.

The power spectral density of process noise $\sigma = 0.5\,\mathrm{m}^2/\mathrm{s}^3$.

$\sigma_1 = \sigma_2 = \sigma_3 = \sigma_\beta = 1\mathrm{mrad}$ is measurement noise standard deviation.

In order to assess the performance of the tracking algorithms, three different metrics are used. The first is the root-mean square error (RMSE), defined as

$$\mathrm{RMSE}_k = \sqrt{\frac{1}{N_M}\sum_{l=1}^{N_M}\left\|\mathbf{x}_k^l - \hat{\mathbf{x}}_k^l\right\|^2} \tag{45}$$

where $\mathbf{x}_k^l$ and $\hat{\mathbf{x}}_k^l$ denote the true and estimated target state value at time k at the l-th MC run, N_M is the total number of independent MC runs.

The second metric is the root time averaged mean square (RTAMS) error, defined as

$$\mathrm{RTAMS} = \sqrt{\frac{1}{t_{\max}N_M}\sum_{k=1}^{t_{\max}}\sum_{l=1}^{N_M}\left\|\mathbf{x}_k^l - \hat{\mathbf{x}}_k^l\right\|^2} \tag{46}$$

where $t_{\max}$ is the total number of time epochs. RTAMS can be used to evaluate the overall performance.

The third metric is the efficiency parameter η defined as

$$\eta = \frac{\mathrm{CRLB}(\mathrm{RTAMS})}{\mathrm{RTAMS}} \times 100\% \tag{47}$$

From the above equation, it can be observed that η indicates "closeness" to the CRLB.

Each group of simulations are carried out on the same target tracks, regardless of the initial convergence period, that is, the target tracking period is set as $40 \le k \le 100$. The number of simulations is set to N_M=2000 . All simulations are implemented on the same processor (Intel(R) Core(TM) i7-7500U CPU 2.70GHz) using MATLAB.

A. Overall performance

This group of simulations aims to compare overall performance of the algorithms. Fig. 1 and Fig. 2 respectively show the RMSE and CRLB of the position and velocity estimation for each algorithm at each time. Table 1 shows the comparison of RTAMS and η of the position and velocity estimation for the algorithms. Table 2 shows the comparison of the averaged runtime of the algorithms at each time.

From Fig. 1, Fig. 2 and Table 1, it can be observed that the DM-IEKF has better precision than the DM-EKF, due to the modification. The target tracking error of the DM-UKF is smaller than that of the DM-IEKF because DM-UKF approximates the statistics of state variables by selecting a series of symmetrical deterministic sampling points. The DM-PLKF shows a very poor RMSE performance at both the position and velocity estimation as a consequence of its severe bias performance. The DM-IPLKF significantly outperforms the DM-PLKF in terms of the RMSE performance, since DM-IPLKF compensates the pseudolinear bias. Specifically, the DM-IVPLKF exhibits the best RMSE performance, due to that DM-IVPLKF uses instrumental vector to further weaken the influence of pseudolinear bias. The efficiency parameter of DM-IVPLKF is the largest, and the target state estimation of DM-IVPLKF is the closest to CRLB.

As can be seen from Table 2, the DM-IEKF is 11% slower DM-EKF, due to the extra computation for the iterative step. The DM-UKF has the largest computational complexity, and takes about three times as long as DM-EKF, since it needs to select sampling points. The runtime of DM-PLKF is 7% less than that of DM-EKF. The DM-IPLKF takes 13% more time than DM-PLKF, due to the extra computation for the bias compensation step. Specifically, the DM-IVPLKF is 19% slower than the DM-IPLKF, because it needs to complete the relevant calculation of instrumental vector.

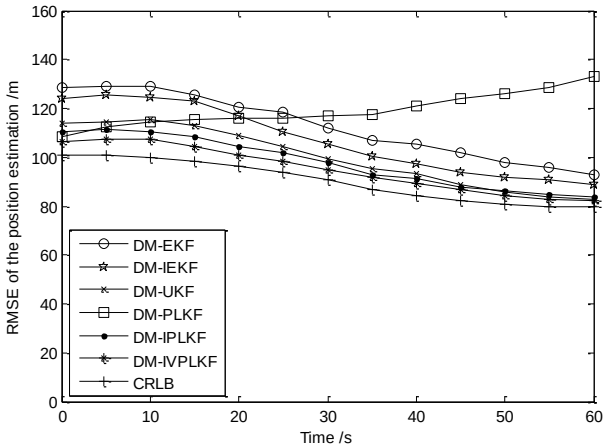

Figure 1. The RMSE of the position estimation versus time.

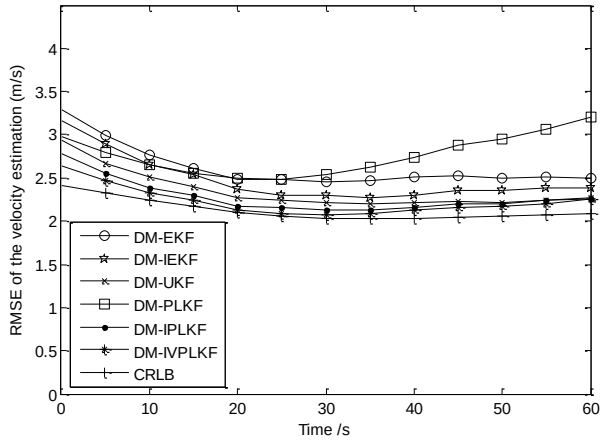

Figure 2. The RMSE of the velocity estimation versus time.

Table 1. Performance Comparison

Algorithm/ CRLB	Position estimation		Velocity estimation	
	RTAMS(m)	η	RTAMS(m/s)	η
DM-EKF	113.4447	79.68	2.6102	81.21
DM-IEKF	107.9506	83.73	2.4708	85.79
DM-UKF	100.7753	89.69	2.3434	90.45
DM-PLKF	119.3649	75.73	2.7489	77.11
DM-IPLKF	98.4613	91.8	2.2704	93.36
DM-IVPLKF	95.7343	94.42	2.215	95.7
CRLB	90.3877	100	2.1197	100

Table 2. Averaged runtime (ms)

Algorithm	DM-EKF	DM-IEKF	DM-UKF
Runtime	0.3469	0.3842	1.0809
Algorithm	DM-PLKF	DM-IPLKF	DM-IVPLKF
Runtime	0.3215	0.3634	0.4316

B. Tracking performance versus measurement noise

This set of simulations examines the performance of the considered filtering algorithms as a function of measurement accuracy. Nine different measurement noise standard deviations σ_n are set, as shown in Table 3. Fig. 3 and Fig. 4 show the RTAMS error of position and velocity estimation for different σ_n respectively.

Table 3. Measurement noise standard deviation (mrad)

σ_n	1	1.5	2	2.5	3	3.5	4	4.5	5

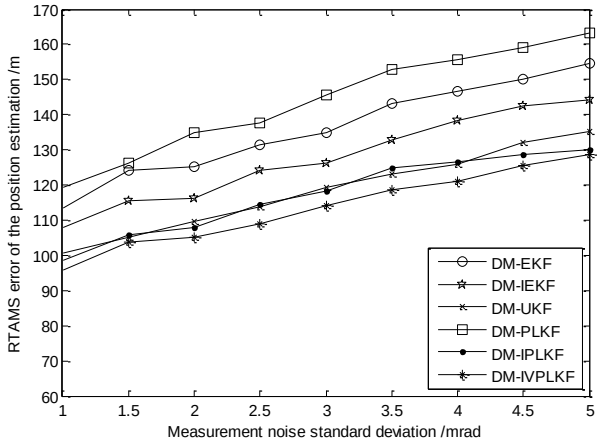

Figure 3. RTAMS error of the position estimation versus the bearing measurement accuracy

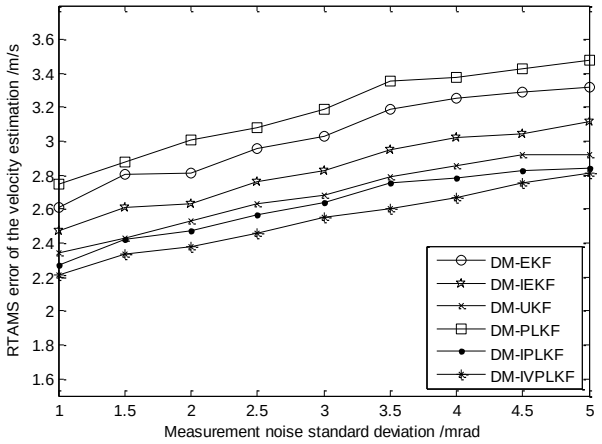

Figure 4. RTAMS error of the velocity estimation versus the bearing measurement accuracy

As expected, it can be observed that a degradation in performance as σ_n is increased. For DM-IVPLKF, the RTAMS error of position estimation is increased by 34% and the RTAMS error of velocity estimation is increased by 27% as σ_n is increased from 1mrad to 5mrad. In this study, the DM-IVPLKF achieves the best performance. The performance of the DM-PLKF is the worst in this set of simulations.

Table 4 and Table 5 list the improvement in performance of the position and velocity estimation relative to a baseline filtering algorithm that is chosen to be the DM-PLKF for $\sigma_n = 4.5\text{mrad}$. Thus, the improvement factor is defined as

$$\text{IF} = \frac{\text{RTAMS}(\text{DM-PLKF}) - \text{RTAMS}(\text{filter})}{\text{RTAMS}(\text{DM-PLKF})} \times 100\% \quad (48)$$

It can be seen that the overall performance in the position and velocity estimation of the proposed DM-IVPLKF achieves 21% and 19% improvement over the DM-PLKF , respectively. The DM-IVPLKF algorithm exhibit a significant performance improvement over the conventional DM-PLKF, DM-EKF, DM-IEKF, DM-UKF, and DM-IPLKF algorithms.

Table 4 Improvement factor of the position estimation

Algorithm	DM-PLKF	DM-EKF	DM-IEKF
IF	0	6%	10%
Algorithm	DM-UKF	DM-IPLKF	DM-IVPLKF
IF	17%	19%	21%

Table 5 Improvement factor of the velocity estimation

Algorithm	DM-PLKF	DM-EKF	DM-IEKF
IF	0	4%	11%
Algorithm	DM-UKF	DM-IPLKF	DM-IVPLKF
IF	15%	17%	19%

V. Conclusions

The distributed filter has become one of the most acclaimed methods for multisensor bearings-only tracking in the presence of clutter interference and missed detections. This article proposed a distributed multisensor fusion pseudolinear Kalman filter algorithm to solve the problems of nonlinear filtering and weak observation of BOT. For each sensor subsystem, the instrumental vector PLKF is used to estimate the target state independently. In the fusion center, the fusion estimation of the target state is obtained by using the multisensor optimal information fusion criterion. Simulations verified that the proposed filter performs accurately and is effective. The main drawback of the kind of PLKF is the biased estimation, which is to be addressed in the future work. We will work on unbiased filtering technology and better multisensor fusion technology.

Acknowledgment

This work was supported by the National Natural Science Foundation of China No.: 62041304 and the National Nature Science Foundation of Ningxia No.: 2021AAC03226. The authors are grateful to the editor and referees for the valuable comments and suggestions.

References

[1] S Hadar, K Itzik. BOTNet: Deep Learning-Based Bearings-Only Tracking Using Multiple Passive Sensors. Sensors (Basel, Switzerland), 2021, 21(13): 1-14.
[2] T Northardt, S C Nardone. Track-before-detect bearings-only localization performance in complex passive sonar scenarios: a case study. IEEE journal of oceanic engineering, 2019, 44(2): 482-491.
[3] X Li, C Zhao, X Lu, et al. Underwater bearings-only multitarget tracking based on modified PMHT in dense-cluttered environment. IEEE Access, 2019, 7: 93678-93689.
[4] J Zhang, H Ji. Modified iterated extended Kalman filter based multi-observer fusion tracking for IRST. Systems Engineering and Electronics, 2010, 32(3):504-507.
[5] A Jawahar, S K Rao. Modified polar extended Kalman filter (MPEKF) for bearings-only target tracking. Indian J. Sci. Technol., 2016, 9(26):1-5.
[6] A Toloei, S Niazi. State estimation for target tracking problems with nonlinear Kalman filter algorithms. Int. J. Comput. Appl., 2014, 98(17):30-36.
[7] D C Chang, M W Fang. Bearing-only maneuvering mobile tracking with nonlinear filtering algorithms in wireless sensor networks. IEEE Syst. J., 2014, 8(1):160-170.
[8] F Daum. Nonlinear filters: Beyond the Kalman filter. IEEE Aerosp. Electron. Syst. Mag., 2005, 20(8):57-69.
[9] N H Nguyen, K Dogancay. Improved Pseudolinear Kalman Filter Algorithms for Bearings-Only Target Tracking. IEEE Transactions on Signal Processing, 2017, 65(23):6119-6134.
[10] H Jiang, Y Cai. Gaussian sum pseudolinear Kalman filter for bearings-only tracking. IET Control Theory & Applications, 2020, 14(3): 452-460.
[11] K Dogancay. 3D pseudolinear target motion analysis from angle measurements. IEEE Trans. Signal Process., 2015, 63(6):1570-1580.
[12] N H Nguyen, K Dogancay. Multistatic pseudolinear target motion analysis using hybrid measurements. Signal Process., 2017, 130: 22-36.
[13] N H Nguyen, K Dogancay. Single-platform passive emitter localization with bearing and Doppler-shift measurements using pseudolinear estimation techniques. Signal Process., 2016, 125: 336-348.
[14] Z Huang,S Chen, C Hao, et al. Bearings-Only Target Tracking with an Unbiased Pseudo-Linear Kalman Filter. Remote Sensing, 2021, 13(15): 2915-2915.
[15] S Bu, A Meng, G Zhou. A New Pseudolinear Filter for Bearings-Only Tracking without Requirement of Bias Compensation. Sensors (Basel, Switzerland), 2021, 21(16): 1-19.
[16] Rao S Koteswara. Bearings-Only Tracking: Observer Maneuver Recommendation. IETE Journal of Research, 2021, 67(2): 193-204.
[17] J Zhang, H Ji. Distributed multi-sensor particle filter for bearings-only tracking. International Journal of Electronics. 2012, 99(2):239-254.
[18] C Han, H Zhu, Z Duan, et al. Multi source information fusion. Beijing: Tsinghua University Press, 2006.
[19] S L Sun, Z L Deng. Multi-sensor optimal information fusion Kalman filter. Automatica, 2004, 40(6): 1017-1023.
[20] S L Sun. Optimal and self-tuning information fusion Kalman multi-step predictor. IEEE Transactions on Aerospace and Electronic Systems, 2007, 43(2): 418-427.
[21] S L Sun. Distributed optimal linear fusion estimators. Information Fusion, 2020, 63:56-73.

Jungen Zhang was born in Jiangxi, China in 1979. He received the B.S. (2001) degree in electronic engineering from the airforce aeronautical university and Ph.D. (2011) degree in pattern recognition and intelligent system from Xidian University, respectively.

Currently, he is a lecturer at the North Minzu University. His primary areas of research have been signal processing, intelligent information processing, passive sensor based targets location and tracking, radar targets recognition and classification. The main published articles are as follows:

[1] Jungen Zhang, Hongbing Ji, Cheng Ouyang. Multitarget Bearings-Only Tracking Using Fuzzy Clustering Technique and Gaussian Particle Filter. The Journal of Supercomputing. 2011, 58(1):4-19.

[2] Jungen Zhang, Hongbing Ji. Distributed multi-sensor particle filter for bearings-only tracking. International Journal of Electronics. 2012, 99(2):239-254.

[3] Jungen Zhang. Bearings-only multitarget tracking based on Rao-Blackwellized particle CPHD filter. International Journal of Circuits, Systems and Signal Processing. 2020, 14:1129-1136.

Shanglin Yang was born in Ningxia, China in 1984. He received his B.S. degree from Northwest A&F University in 2007, and his M.S. and Ph.D. degrees from Northwestern Polytechnical University, in 2009 and 2016, respectively. Since 2016, he has been a lecturer at North Minzu University, China. His research interests are in MEMS and magnetic sensors. (Corresponding author: ysl029@163.com)

Contribution of Individual Authors to the Creation of a Scientific Article (Ghostwriting Policy)

Jungen Zhang was responsible for the algorithm research and the optimization.
Shanglin Yang carried out the simulation and analysis.

Sources of Funding for Research Presented in a Scientific Article or Scientific Article Itself

This work was supported by the National Natural Science Foundation of China No.: 62041304 and the National Nature Science Foundation of Ningxia No.: 2021AAC03226.